SEMARAK ILMU PUBLISHING

Semarak International Journal of Material Research

Journal homepage:
https://semarakilmu.my/index.php/sijmr/index
ISSN: 3083-8908

Comparative Analysis of Hot Face and Internal Insulators using X-Ray Diffraction (XRD): Element & Compound Analysis for Thermal Applications

Tew Heng Yao[1], Azzura Ismail[1,*]

[1] Faculty of Mechanical and Manufacturing Engineering, Universiti Tun Hussein Onn, Malaysia

ARTICLE INFO

Article history:
Received 20 April 2025
Received in revised form 21 May 2025
Accepted 9 June 2025
Available online 30 June 2025

Keywords:
Insulation materials; hot face insulator; internal insulator; XRD analysis; crystalline phases; microstructural; thermal stability; resistance; petrochemical; secondary reformer

ABSTRACT

Insulation materials are essential for maintaining the longevity and effectiveness of thermal systems, especially in high-temperature settings like industrial furnaces and petrochemical plants. Using X-ray diffraction (XRD) techniques, this study compares the microstructural characteristics of internal and hot face insulators. The goal is to assess these materials' phase composition, and microstructural integrity, all of which have a direct impact on their longevity and thermal performance. The hot face and internal insulators' phases and microstructural configurations differed significantly, as shown by XRD analysis, underscoring their individual resistance to chemical and thermal stress. The hot face insulator was appropriate for direct heat exposure since it displayed phases with improved thermal stability and resilience to high-temperature deterioration. On the other hand, within layered systems, the internal insulator showed a structure optimal for thermal insulation and resilience to thermal cycling. Both insulators function directly within the secondary reformer of a petrochemical process.

1. Introduction

Controlling heat transfer is strongly related to the idea of thermal insulation. Essential details on the parts, goods, and materials used in thermal insulation. Thermal insulation materials are intended to reduce a system's susceptibility to heat transmission, according to the ISO standard [1]. The purpose of thermal insulation materials is to lessen heat transfer between an object and its environment. Numerous uses, including high-temperature industrial processes and building construction, require these materials. In the building sector, there are several reasons why thermal insulation materials are used to reduce energy consumption and vibration, to maintain a constant medium temperature inside the insulated object and temperature changes from outside, heat distortion of the insulated object and to reduce vibration as well as to reinforce structures [2-4].

Heat exchangers, tanks, and pipes are all depend heavily on thermal insulation, which has long been a vital part of industrial and installation systems. In addition to these uses, the building, power

* *Corresponding author.*
E-mail address: azzura@uthm.edu.my

https://doi.org/10.37934/sijmr.3.1.920

generating, chemical processing, refrigeration, firefighting, and aerospace sectors all make extensive use of it [5-8]. The hot face insulator, seen in Figure 1(a), is intended to limit energy loss, preserve overall efficiency, and retain heat within the system. It must endure harsh conditions because it is positioned just inside the burners' high-temperature zone. This insulator can withstand temperatures above 1800°C because it is composed of high-purity concrete that has very little iron or silica. A further thermal barrier that lowers heat loss and boosts energy efficiency is the internal insulator, which is seen in Figure 1(b). This low-iron insulating castable insulator, which is intended to function at temperatures as high as 1400°C, is applied to the inner surfaces of the burner walls. Usually, casting is used for installation, guaranteeing adequate coverage and longevity.

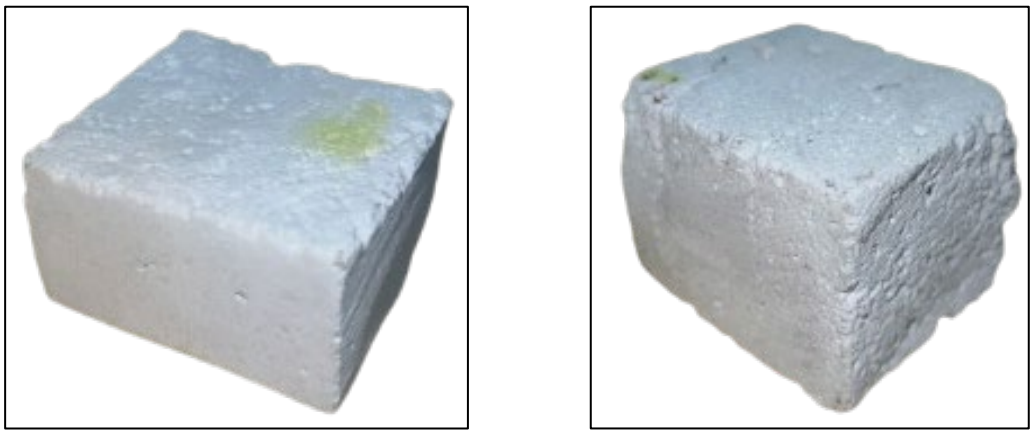

(a) (b)

Fig. 1. Reformer clay (a) Hot Face Insulator (b) Internal Insulator

The insulators in this study are used in petrochemical facilities' secondary reformers. The conversion of hydrocarbons into synthesis gas is facilitated by this reformer, which is essential to the manufacturing of ammonia. The secondary reformer can normally tolerate the temperatures between 800°C and 1400°C [9] and pressures between vacuum and 1000 bar while operating in harsh environments [10]. With sophisticated burners and refractory materials, this catalytic reactor is specially developed to guarantee effective chemical reactions.

The secondary reformer has a burner system that allows for adequate reactant mixing, as shown in Figure 2 [11]. The three main processes in the process are steam methane reforming, which turns methane into synthesis gas over a catalyst bed, burning hydrocarbons to supply the heat required for additional reactions, and mixing process gas with air to establish a consistent reaction environment. The efficiency and dependability of the secondary reformer in industrial applications are guaranteed by the combination of high-temperature operation, refractory materials, and sophisticated burner design.

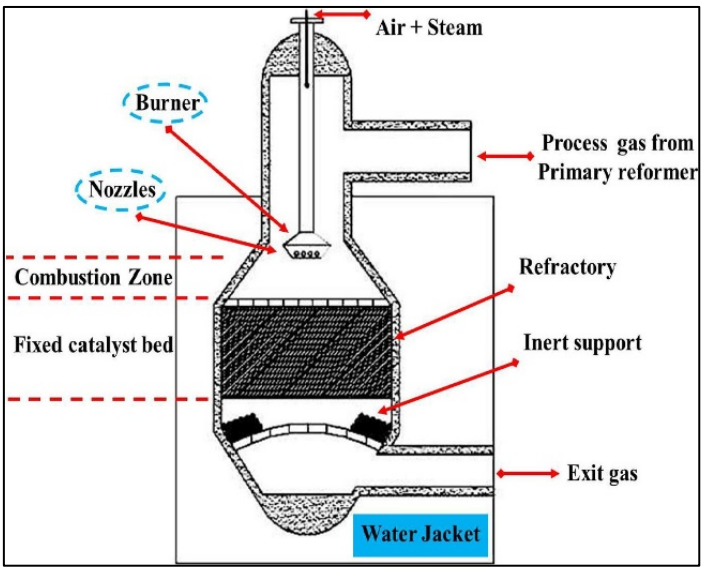

Fig. 2. Secondary reformer schematic illustration [11]

2. Methodology

X-ray diffraction (XRD) was used to identify the phases and compounds of hot face and internal insulators. The sample is exposed to incident X-rays in order to measure the scattering angles and intensities of the X-rays that interact with the material. Plotting the results diffraction pattern as intensity versus scattering angle enables structural analysis and phase identification. Critical information about the material's crystal structure, internal tensions, and possible flaws can be obtained by analysing the locations and intensities of the diffraction peaks. This method can also be used to identify departures from the ideal lattice structure brought on by contamination, mechanical stress, or heat exposure [12–14].

Wide-Angle X-ray Diffraction (WAXD) is a subset of the more general X-ray scattering techniques, including X-ray diffraction (XRD), which depends on the diffraction of X-rays. These techniques analyse material structures using X-ray beams that are elastically dispersed [15]. Small Angle X-ray Scattering (SAXS), which involves incident X-rays on the sample across a narrow angle range of 0.1-100, is another elastic scattering-based X-ray technique. SAXS uses X-ray reflection to quantify the thickness, roughness, and density of thin films and detects structural correlations at scales of several nanometers or bigger (such crystal superstructures). The angular range covered by WAXD is greater than 100 [16, 17].

The relationship between crystal structure and the locations of the diffracted peaks When X-rays with small enough wavelengths interact with a crystal lattice, the lattice points cause them to be diffracted. These diffracted waves experience constructive interference at particular angles of incidence, which causes the diffraction pattern to produce discrete intensity peaks. Bragg's Law, which establishes the essential link between the incident X-ray wavelength, the diffraction angle, and the distance between atomic planes in the crystal structure, provides a mathematical description of this event. The following is the related equation [18].

Miller indices are a set of three integers that constitute a notation system for identifying directions and planes within crystals. For directions, the [*h k l*] Miller indices represent the normalized difference in the respective *x*, *y* and *z* coordinates (in a Cartesian coordinate system) of two points along the direction. For planes, the Miller indices (*h k l*) of a plane are simply the *h k l* values of direction perpendicular to the plane [19]. The experiment process was summarized in the flowchart shown in Figure 3.

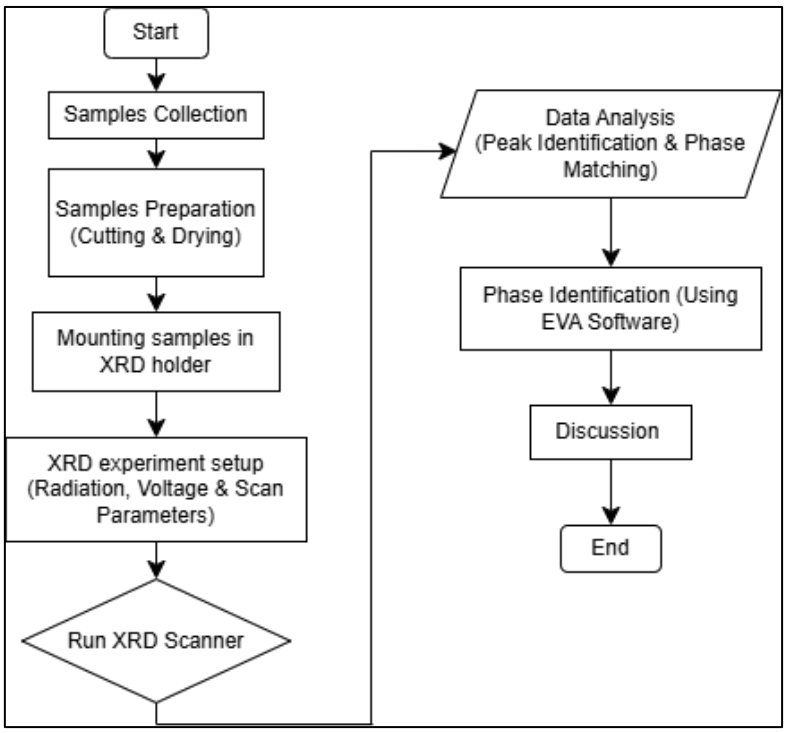

Fig. 3. Flowchart for the research of Hot Face Insulator and Internal Insulator using XRD Analysis

2.1 Sample Cutting & Drying

Both internal and hot face insulator samples were subjected to a methodical cutting into millimetres dimensions and drying procedure to guarantee accurate characterization via XRD analysis. This procedure is essential for preserving the materials' structural integrity and getting rid of any moisture or impurities that might have affected the analysis. To reduce mechanical stress and structural damage, the insulating materials were chopped into the proper sizes (which is 20 mm x 20 mm x 10 mm) using an abrasive cutter or diamond saw. The initial step in the cutting procedure was marking the sample, which involved labelling the insulator with the dimensions for analysis. Then, to prevent creating microcracks or changing the microstructure, precise cutting was carried out using a low-speed diamond saw. The edges, particularly the surface to be examined, were delicately polished to eliminate imperfections without changing the internal phase structure.

After cutting, the samples were dried to eliminate any remaining moisture that would have impacted phase identification and XRD peak intensities. The samples were dried by placing them in a drying oven set at 110°C for 24 hours to remove any remaining moisture. To avoid changing the phases, the temperature was meticulously regulated and allowed to cool gradually avoid causing thermal stress on the insulator materials.

As the samples were being prepared for microstructural and phase examination by XRD, this cutting and drying technique made sure they maintained their original state. In addition to reducing contamination, the meticulous handling produced accurate data for evaluating insulation effectiveness under hot conditions.

2.2 Mounting Samples into XRD holder

The internal and hot face insulator samples stayed in their cubic shape during the cutting and drying operation. Then carefully placed in the XRD holder, accurate phase identification and

microstructural analysis free of artifacts and misalignment depended on proper mounting. To get accurate diffraction results, extra careful to the materials' orientation and surface preparation. To avoid contamination, the samples were then cleaned using ethanol wipes or compressed air to get rid of any remaining dust or debris from handling and cutting.

The XRD holder shown in Figure 4 was used to install the cubic insulator samples since XRD measurements depend on exact alignment. To guarantee the best diffraction findings, the cubic samples were positioned in the holder with the flattest face facing the X-ray beam to prevent the cubic samples from sliding while scanning.

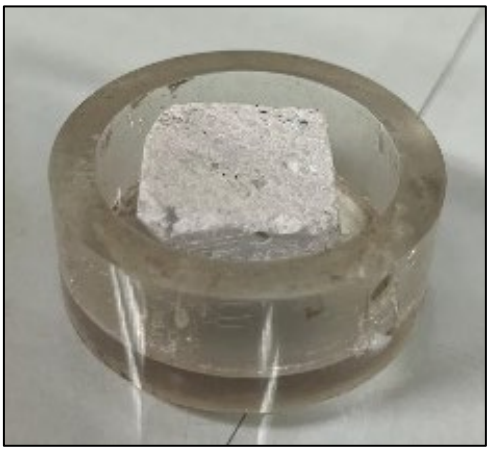

Fig. 4. Sample mounted in XRD holder

The orientation of the sample properly aligns with the X-ray beam to make sure reliable data collection. The sample was examined for stability to avoid tilting or movement during the scan, and the XRD equipment was calibrated using a common reference material. Subsequently, the internal insulator and cubic hot face insulator samples were appropriately positioned within the XRD apparatus, guaranteeing accurate microstructural investigation and phase identification.

2.3 X-ray Diffraction Experiment Setup (Radiation, Voltage and Scan Parameters)

The X-ray diffraction (XRD) experiment was performed to examine the crystalline structure and phase composition of the internal insulator and hot face insulator. Precise calibration, sample alignment, and data analysis utilizing EVA software for phase detection were all part of the experiment design. X-ray diffractometer (see Figure 5) using the source of Cu-Kα radiation (λ = 1.5406 Å), by penetration and diffraction signals. To produce a steady X-ray beam, the device was run at 40kV of voltage and 30mA of current.

The diffraction peaks of ceramic or refractory phases, the scanning parameters with the scan range (2θ) are 10° to 80°. The step size, which is 1° per minute, is then modified based on sample size to maximize beam width and resolution while balancing data quality and acquisition time. For maximum accuracy, the XRD equipment was calibrated using a common reference material like silicon or corundum and reduce inaccuracies, baseline corrections and background noise can be reduced.

Fig. 5. X-ray Diffractometer (XRD BRUKER D8 ADVANCE)

2.4 XRD Scanning Process for Hot Face and Internal Insulator

For optimal accuracy, the XRD equipment was switched on a few minutes prior to scanning due to the X-ray tube was warmed to ensure system stability and prevent intensity changes. After making sure the sample holder was correctly oriented with the X-ray beam, it was placed inside the XRD chamber. The detector and X-ray tube were set up to produce and gather diffracted X-rays at various angles. As soon as the scan began (Figure 6), the device began to spin the sample and gather diffraction data.

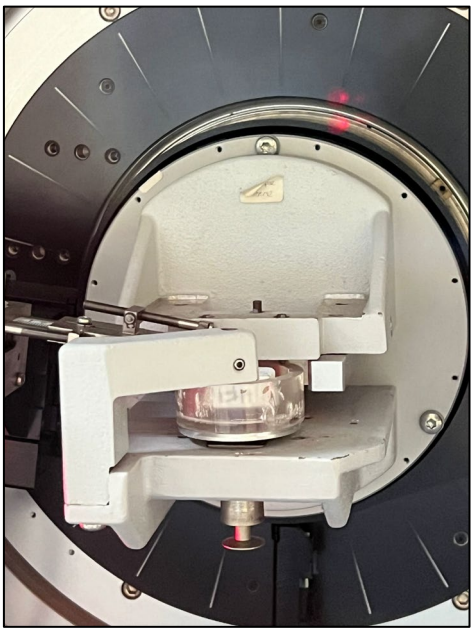

Fig. 6. Insulator scanning process

Diffraction peaks were found and recorded as a result of constructive interference at particular angles created by the X-ray beam's interaction with the sample (Bragg's Law). Depending on the scan

speed and range, each sample took between 30 to 60 minutes to complete. The raw diffraction pattern (intensity vs. 2θ) was saved in a suitable format when the scan was finished. EVA software was used to process data, which included peak detection using the ICDD PDF-4 database for phase matching and background correction to eliminate noise. Next, compare the phases of the internal insulator and the hot face to examine contamination and effect temperature. To ensure accurate phase identification by XRD scan, the internal insulators and hot face were compared to access their thermal stability and microstructural integrity.

3. Results

The phase composition, microstructural integrity, and thermal stability of the internal and hot face insulation materials utilized in the petrochemical reformer were examined using X-ray diffraction analysis. Evaluating these materials' microstructural integrity, phase composition, and crystalline behaviour was the main goal because these factors have a direct impact on their durability and thermal performance. EVA software was used to analyse the acquired diffraction patterns, enabling phase identification and crystalline size calculation. The analysis's main goals were to find the main refractory phases, spot any potential phase changes, and assess the materials' thermal stability. The findings focus on the insulation system's performance, especially about the phase retention, structural stability, and possible long-term deterioration impacts. To comprehend the variations in peak strength, broadening, and phase composition between the internal and hot face insulators, the diffraction patterns were analysed. These differences are covered in depth in the sections that follow in Figure 7 to 10.

3.1 Phase Identification and Comparison

The XRD diffraction pattern provided insight into the phases present in both insulation materials, revealing variations in phase composition between the hot face insulator and internal insulator due to their differing exposure conditions (Table 1). Firstly, phase identification based on the hot face insulator sample 1 (Figure 7) and sample 2 (Figure 8) shows the main phases included the Corundum (Al_2O_3) which commonly found in refractory materials contributing to high-temperature resistance. Quartz or Cristobalite (SiO_2) is silica-based phases that may influence thermal behaviour. The other compounds detected such as Hibonite which is the high-temperature refractory phase also known as Calcium Aluminium Oxides ($CaAl_{12}O_{19}$) renowned for its exceptional mechanical strength, chemical resistance, and thermal stability. At extremely high temperatures, it maintains its stability, avoiding undesired phase changes that can impair the refractory material's performance.

Table 1
Comparison of Hot Face Insulator Sample 1 and Sample 2

Hot Face Insulator Sample	Compound	Chemical Formula	JCPDS Number	Percentage (%)
Sample 1	Hibonite	$CaAl_{12}O_{19}$	01-076-0665	55.16%
	Corundum	Al_2O_3	01-070-5679	56.53%
	Calcium Aluminum Oxide	$CaAl_{12}O_{19}$	00-007-0085	23.41%
	Cristobalite	SiO_2	00-003-0272	16.80%
Sample 2	Hibonite	$CaAl_{12}O_{19}$	01-076-0665	84.62%
	Corundum	Al_2O_3	01-070-5679	88.88%
	Calcium Aluminum Oxide	$CaAl_{12}O_{19}$	00-025-0122	62.62%
	Quartz	SiO_2	00-002-0459	15.11%

Peak locations and intensity variations are displayed in the graph comparison as the primary findings. Similar peak positions are displayed by both hot face insulator samples, indicating that the phase composition is constant between them. Due to the identical temperature exposure, the peak broadening for the two hot face samples then seemed to be rather similar.

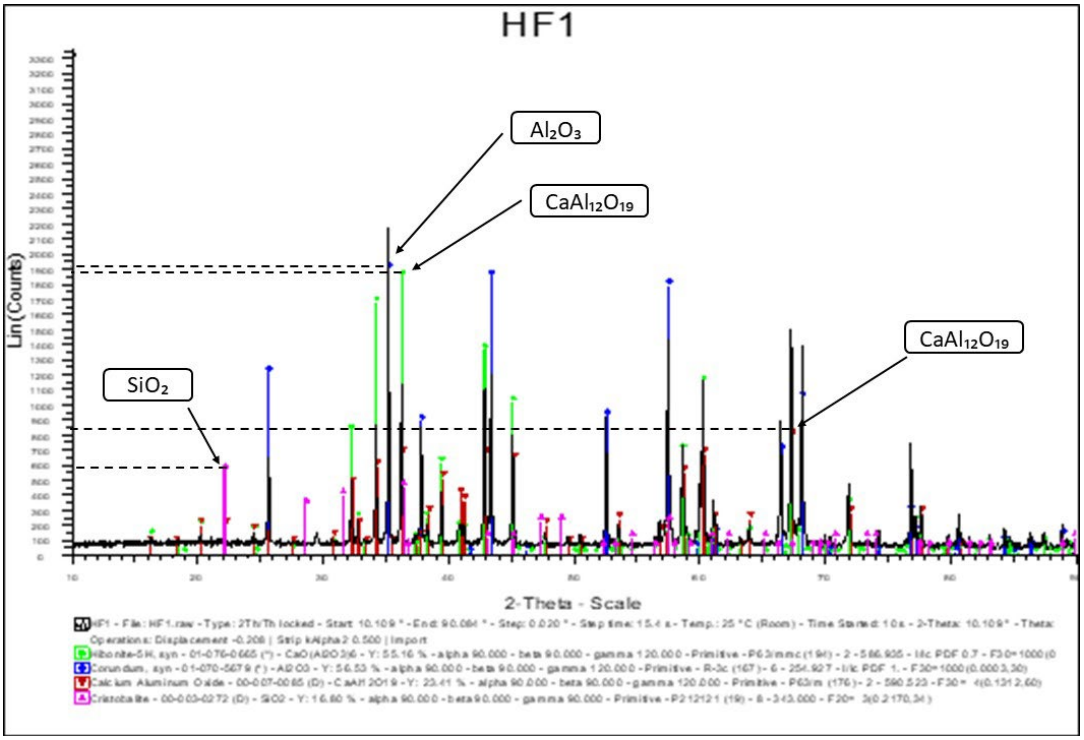

Fig. 7. Hot Face Insulator (Sample 1)

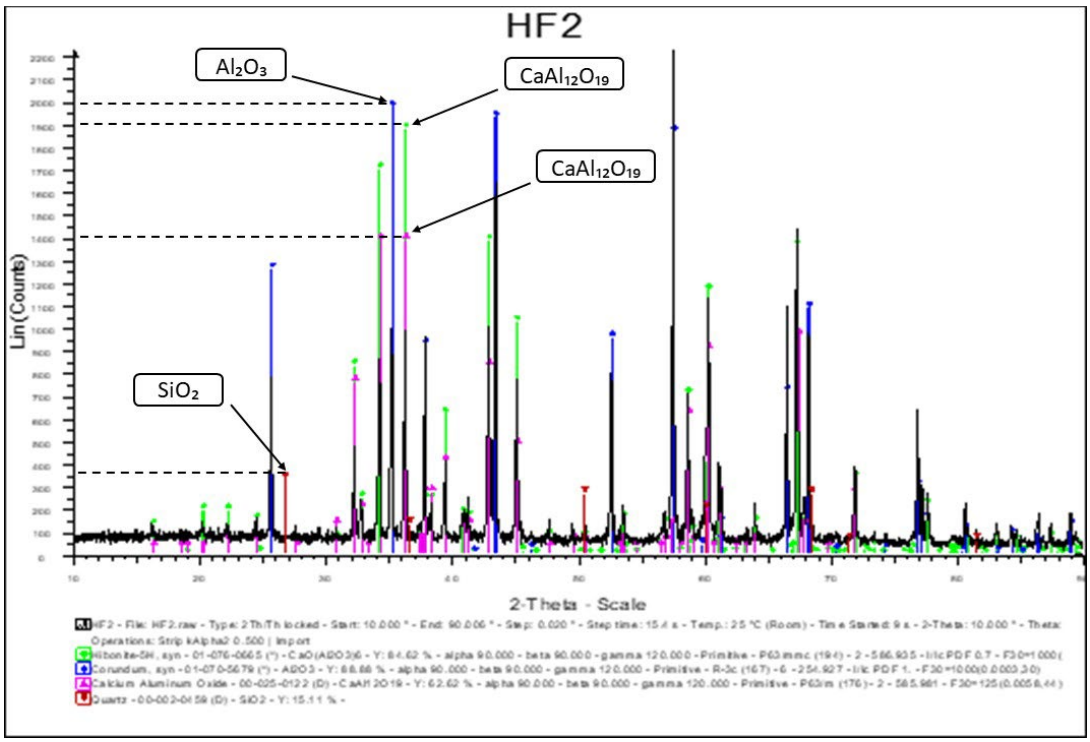

Fig. 8. Hot Face Insulator (Sample 2)

Secondly, the internal insulator samples 1 (Figure 9) and 2 (Figure 10) used for phase identification reveal that the main phases comprise aluminium oxide (AlO_3), also known as alumina, which is the principal component of refractory materials and is renowned for its strong thermal resistance (Table 2). It indicates that the interior insulator is made to resist high temperatures. There are several crystalline forms of silica or quartz (SiO_2). The insulator's mechanical characteristics and thermal expansion are influenced by the presence of silica phases. Apart from that, potential impurities or secondary phases brought on by the high-temperature reactions could be oxides based on calcium or iron. Mechanical integrity and thermal stability may be impacted by the presence of Fe-based oxides.

Major phases (AlO_3 and SiO_2) are present in both internal insulator samples; however, the distribution of minor phases and peak intensities varies, suggesting potential structural or compositional variations. The phases of calcium aluminium oxide were also discovered, which helped to explain the material's tolerance to high temperatures. The disparities in peak intensities point to changes in grain size, crystallinity, or past heat exposure.

Table 2
Comparison of Internal Insulator Sample 1 and Sample 2

Internal Insulator Sample	Compound	Chemical Formula	JCPDS Number	Percentage (%)
Sample 1	Aluminium Oxide	Al_2O_3	01-075-1865	60.60%
	Corundum	Al_2O_3	01-070-5679	26.11%
	Hibonite	$CaAl_{12}O_{19}$	01-076-0665	46.64%
	Calcium Aluminum Oxide	$CaAl_{12}O_{19}$	00-007-0085	26.22%
	Silicon Oxide	SiO_2	01-073-3434	28.37%
Sample 2	Hibonite	$CaAl_{12}O_{19}$	01-075-1865	79.90%
	Corundum	Al_2O_3	01-070-5679	103.36%
	Calcium Aluminum Oxide	$CaAl_{12}O_{19}$	00-007-0082	15.37%
	Quartz	SiO_2	01-073-3439	37.81%

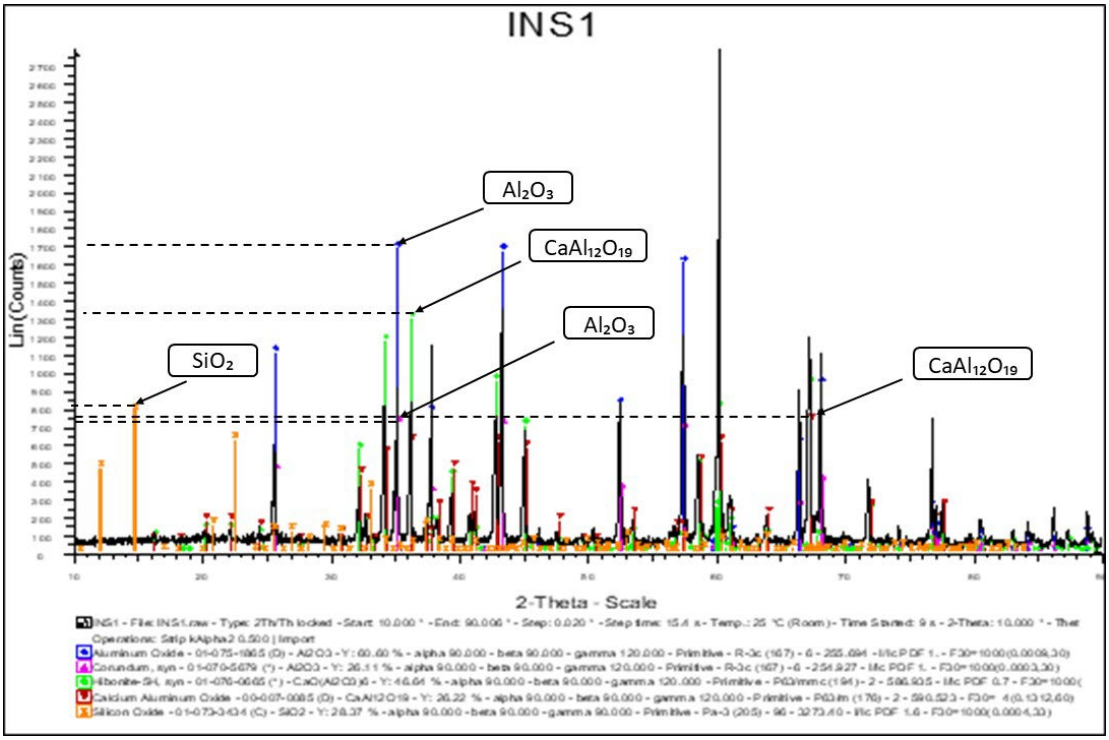

Fig. 9. Internal Insulator (Sample 1)

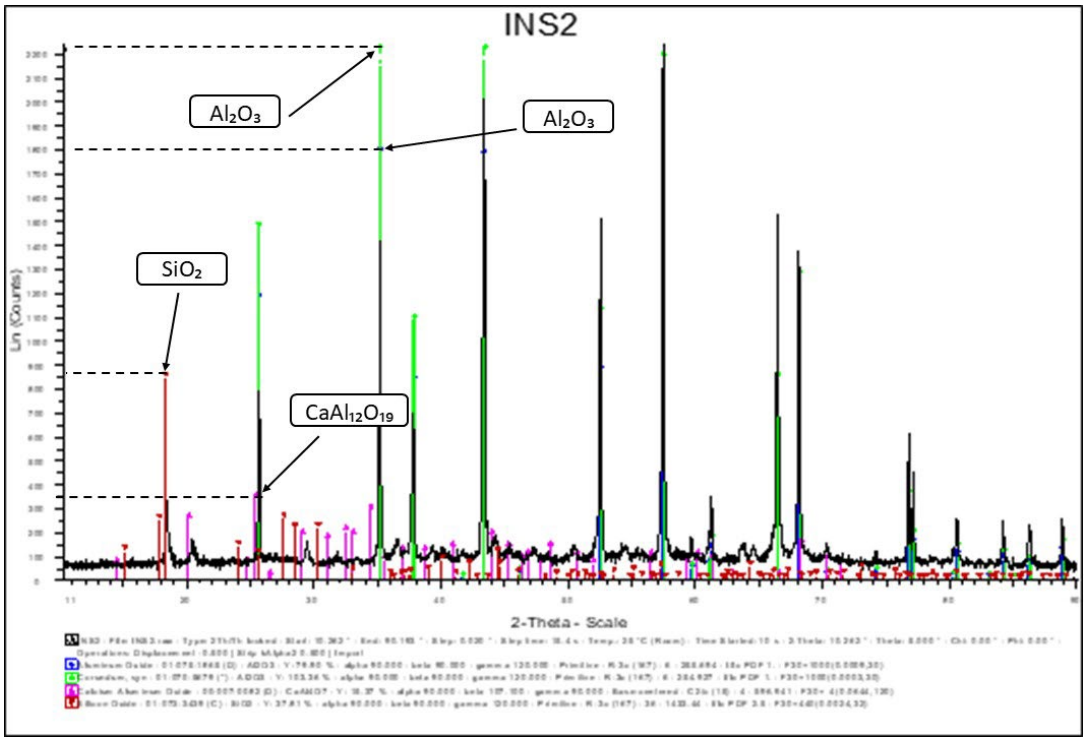

Fig. 10. Internal Insulator (Sample 2)

The hot face insulator and internal insulator's phase composition and thermal stability were all significantly disclosed by the X-ray diffraction (XRD) investigation (Table 3). Alumina and silica-based compounds were the main constituents of both insulators, according to the diffraction patterns, the hot face insulator showed bigger crystallites and shaper peaks, suggesting superior thermal stability. The internal insulator, on the other hand, displayed wider peaks and minor structural changes, which may indicate that the grain was refined or amorphized as a result of extended heat cycling. Notwithstanding these little variations, neither material showed any signs of contamination, indicating that they are both chemically stable under operating circumstances. The observed changes in peak intensity and widening imply that the internal insulator may have undergone minor phase transitions over time, while the hot face insulator is still structurally intact. These results are essential for evaluating the insulation materials' long-term performance and degradation mechanisms in high-temperature petrochemical reformers.

Table 3
Comparison of Hot Face and Internal Insulators

Parameter	Hot Face Insulator	Internal Insulator
Primary Phases	Mullite, Corundum, Silica	Mullite, Silica-based phases
Crystallite Size	Larger, well-defined	Smaller, broad peaks
Peak Broadening	Minimal	Moderate, indicating microstructural changes
Phase Stability	High	Slight phase modifications observed
Contamination	None detected	None detected

4. Conclusions

The objective of this work is to assess these materials' microstructural integrity, phase composition, and crystalline behaviour using X-ray diffraction (XRD) analysis. These factors have a

direct impact on the materials' durability and thermal performance. The hot face and internal insulators' crytalline phases and microstructural configurations differed significantly, as shown by XRD analysis, underscoring their individual resistance to chemical and thermal stress. Finding the main refractory phases and identifying any potential phase transitions were the main goals of the investigation. and assessing the materials' thermal stability. Significant phase discrepancies between the two insulators were found in the results, suggesting changes in thermal stability and possible degradation mechanisms.

i. The absence of mullite and the presence of notable phase transitions in the hot face insulator are strong indicators of high-temperature deterioration. This results in weakened mechanical properties and compromised thermal stability, especially in areas directly exposed to extreme heat.
ii. The internal insulator exposed to low heat, so it maintained a more stable phase composition.
iii. Phases of calcium aluminium oxide were found in both insulators, which may have improved thermal stability and contributed to the material's tolerance to high temperatures.
iv. The presence of hibonite in the hot face insulator indicates that the materials are designed to have improved chemical and heat resistance. However, the internal insulator is differently because it is not subjected to the same thermal stress.
v. The observed changes in peak intensity and widening imply that the internal insulator may have undergone minor phase transitions over time, but the hot face insulator still structurally intact.

The diffraction patterns verified that silica-based and aluminum-based compounds were the main constituents of both insulators. Better thermal stability is shown by the hot face insulator's bigger crystallites and sharper peaks. The internal insulator, on the other hand, displayed wider peaks and minor structural changes, which may indicate that the grain was refined or amorphized as a result of extended heat cycling. All things considered, these results show how the two forms of insulation degrade differently, highlighting the necessity of material optimization to improve longevity and efficiency in petrochemical reformer applications.

Further research is required to optimize the composition of refractory materials for increased durability and thermal efficiency, as these findings also shed important light on the materials' long-term performance under challenging working conditions. SEM-EDX analysis may be used in future research to examine microstructure and evaluate microstructural alterations at a finer scale. Finally, the findings show that although both materials retain adequate heat resistance, the internal insulator might need to be checked on a regular basis to guarantee peak performance over long service periods.

Acknowledgement
This research was supported by Universiti Tun Hussein Onn Malaysia (UTHM) through GPPS (Vot. Q657). The author would like to thank the Faculty of Mechanical Engineering and Manufacturing, Universiti Tun Hussein Onn Malaysia for providing the necessary research facilities for this study.

References

[1] Abdullaev, Azim Rasulovich, and Isroiljonova Nizomjon Qizi Zulxumor. "A Review On: Analysis Of The Properties Of Thermal Insulation Materials." *The American Journal of Interdisciplinary Innovations and Research* 3, no. 05 (2021): 27-38. https://doi.org/10.37547/TAJIIR/VOLUME03ISSUE05-06

[2] Pásztory, Zoltán. "An overview of factors influencing thermal conductivity of building insulation materials." *Journal of Building Engineering* 44 (2021): 102604. https://doi.org/10.1016/J.JOBE.2021.102604

[3] Aditya, Lisa, TM Indra Mahlia, Behzad Rismanchi, H. M. Ng, M. H. Hasan, H. S. C. Metselaar, Oki Muraza, and H. B. Aditiya. "A review on insulation materials for energy conservation in buildings." *Renewable and sustainable energy reviews* 73 (2017): 1352-1365. https://doi.org/10.1016/J.RSER.2017.02.034

[4] Abdullaev, Azim Rasulovich, and Isroiljonova Nizomjon Qizi Zulxumor. "A Review On: Analysis Of The Properties Of Thermal Insulation Materials." *The American Journal of Interdisciplinary Innovations and Research* 3, no. 05 (2021): 27-38. https://doi.org/10.37547/TAJIIR/VOLUME03ISSUE05-06

[5] Chaturvedi, Kamna, Manish Dhangar, Ayushi Jaiswal, Avanish Kumar Srivastava, and Sarika Verma. "The uniqueness of flexible and mouldable thermal insulation materials in thermal protection systems—A comprehensive review." *The Canadian Journal of Chemical Engineering* 102, no. 10 (2024): 3372-3390. https://doi.org/10.1002/cjce.25278

[6] Gunnarshaug, Amalie, Maria Monika Metallinou, and Torgrim Log. "Study of industrial grade thermal insulation at elevated temperatures." *Materials* 13, no. 20 (2020): 4613. https://doi.org/10.3390/ma13204613

[7] Khaziakhmetova, E. R. "Application of thermal insulation materials in production and safety." *Occupational Health and Safety in Industrial Enterprises* 10 (2020): 53-59. https://doi.org/10.33920/pro-4-2010-06

[8] Bahadori, A. "Design and application of thermal insulation." *Thermal insulation handbook for Oil, Gas, Petrochemical Industries, 1st edition, Elsevier Inc* (2014). https://doi.org/10.1016/B978-0-12-800010-6.00001-0

[9] Kuleshova, Evgenia, Ivan Fedotov, Dmitriy Maltsev, Svetlana Fedotova, Georgiy Zhuchkov, and Alexander Potekhin. "Phase Formation Features of Reactor Pressure Vessel Steels with Various Ni and Mn Content under Conditions of Neutron Irradiation at Increased Temperature." *Metals* 13, no. 4 (2023): 654. https://doi.org/10.3390/met13040654

[10] Phan, Anh D., Kajetan Koperwas, Marian Paluch, and Katsunori Wakabayashi. "Coupling between structural relaxation and diffusion in glass-forming liquids under pressure variation." *Physical Chemistry Chemical Physics* 22, no. 42 (2020): 24365-24371. https://doi.org/10.1039/D0CP02761H

[11] Ardali, Alireza Mohammadian, and Behnam Lotfi. "Failure analysis of secondary reformer burner nozzles made from Incoloy 825 in an ammonia production plant." *Engineering Failure Analysis* 118 (2020): 104860. https://doi.org/10.1016/j.engfailanal.2020.104860

[12] Ali, Asif, Yi Wai Chiang, and Rafael M. Santos. "X-ray diffraction techniques for mineral characterization: A review for engineers of the fundamentals, applications, and research directions." *Minerals* 12, no. 2 (2022): 205. https://doi.org/10.20944/preprints202112.0438.v1

[13] Freychet, Guillaume, Eliot Gann, Lars Thomsen, Xuechen Jiao, and Christopher R. McNeill. "Resonant tender x-ray diffraction for disclosing the molecular packing of paracrystalline conjugated polymer films." *Journal of the American Chemical Society* 143, no. 3 (2021): 1409-1415. https://doi.org/10.1021/jacs.0c10721

[14] Dolabella, Simone, Aurelio Borzì, Alex Dommann, and Antonia Neels. "Lattice strain and defects analysis in nanostructured semiconductor materials and devices by high-resolution X-ray diffraction: theoretical and practical aspects." *Small Methods* 6, no. 2 (2022): 2100932. https://doi.org/10.1002/smtd.202100932

[15] Rowolt, Christian, Hannes Fröck, Benjamin Milkereit, Michael Reich, Wolfgang Kowalski, Andreas Stark, and Olaf Keßler. "In-situ analysis of continuous cooling precipitation in Al alloys by wide-angle X-ray scattering." *Science and technology of advanced materials* 21, no. 1 (2020): 205-218. https://doi.org/10.1080/14686996.2020.1739554

[16] Nepal, Prakash, Abdullah Al Bashit, Lin Yang, and Lee Makowski. "Small-angle X-ray microdiffraction from fibrils embedded in tissue thin sections." *Applied Crystallography* 55, no. 6 (2022): 1562-1571. https://doi.org/10.1101/2022.05.10.491381

[17] Kawamukai, Honoka, Shumpei Takishita, Kazumi Shimizu, Daisuke Kohda, Koichiro Ishimori, and Tomohide Saio. "Conformational distribution of a multidomain protein measured by single-pair small-angle x-ray scattering." *The Journal of Physical Chemistry Letters* 15, no. 3 (2024): 744-750. https://doi.org/10.1021/acs.jpclett.3c02600

[18] Cantor, Brian. *The equations of materials*. Oxford University Press, 2020. https://doi.org/10.1093/oso/9780198851875.003.0002

[19] Sun, Shaodong, Xiaochuan Zhang, Jie Cui, and Shuhua Liang. "Identification of the Miller indices of a crystallographic plane: a tutorial and a comprehensive review on fundamental theory, universal methods based on different case studies and matters needing attention." *Nanoscale* 12, no. 32 (2020): 16657-16677. https://doi.org/10.1039/d0nr03637d